IEEE Access
Multidisciplinary | Rapid Review | Open Access Journal

Received April 5, 2017, accepted May 17, 2017, date of publication May 26, 2017, date of current version June 27, 2017.

Digital Object Identifier 10.1109/ACCESS.2017.2708760

Towards Differentiated Rate Control for Congestion and Hotspot Avoidance in Implantable Wireless Body Area Networks

MUHAMMAD MOSTAFA MONOWAR, (Member, IEEE), AND FUAD BAJABER
Faculty of Computing and Information Technology, Department of Information Technology, King AbdulAziz University, Jeddah 21589, Saudi Arabia
Corresponding author: Muhammad Mostafa Monowar (mmonowar@kau.edu.sa)

This work was supported by the Deanship of Scientific Research, King AbdulAziz University, Jeddah, under Grant 611-18-D1437.

ABSTRACT Implantable wireless body area networks (WBANs) are gaining considerable attention to the researchers due to their high potential in healthcare applications. However, one of the biggest challenges of WBANs is the heat produced by wireless implants because of the continuous sensing of physiological parameters that could cause thermal impairment to the human tissue. Again, an implantable WBAN can be equipped with heterogeneous nodes having diverse throughput, fidelity, and latency demands. Also, un-controlled traffic reporting rate could cause high contention as well as congestion in nodes, which are usually organized forming a many-to-one routing paradigm in a WBAN. The problem of congestion not only restrains in satisfying the desired QoS requirements of the diverse healthcare applications, but also increases the dissipated energy and the temperature of an implant biosensor. This paper proposes a novel rate control mechanism with the aim of providing a unified solution for both congestion and hotspot avoidance in an implantable WBAN. The proposed scheme also presents a scheduling rate allocation mechanism reflecting the relative priority of biosensors. The performance of the protocol is evaluated using simulations, which demonstrate that the proposed protocol maintains lower temperature rise as well as avoid the creation of hotspot(s). The results also indicate that the proposed protocol significantly improves the performance of healthcare applications in terms of throughput, reliability, latency, as well as energy consumption.

INDEX TERMS Wireless body area networks, rate control, thermal effects, congestion avoidance.

I. INTRODUCTION

Wireless Body Area Networks (WBANs) have been thought of as one of the striking technologies in the health care arena in the last few years. The rapid advancement in Micro-Electro-Mechanical Systems (MEMS) [1] along with low-power wireless networking technologies have paved the way for such proliferation of WBANs. WBANs use low power, tiny, intelligent sensors to provide continuous health monitoring and real time feedback to the health care personnel.

Among numerous potential applications [2], one of the vital applications for WBANs is remote health monitoring that aims to implant biomedical sensors, known as *in-vivo* sensors, inside the human body. The in-vivo sensors detect, record and transmit data regarding any physiological changes in an individual over wireless links to a central coordinator device, usually known as Body Coordinator (BC) [3]. To reduce energy-consumption, the in-vivo sensors usually exploit multi-hop communication through a number of relay nodes to deliver the data toward BC [4]–[6]. As studied in several researches [7], [8], the continuous sensing of in-vivo sensors produces heat due to wireless communication. Such thermal-increase could be extremely dangerous for the neighboring tissues, and if it prolongs for a long time it might damage them [3], [9]. Furthermore, some delicate organs are prone to thermal damage even with modest heating [10].

A number of studies attempted to address the thermal problem of implanted WBANs [3], [11]–[15]. Most of the solutions focused on devising thermal-aware routing protocols in which a node after being heated (termed as ''hotspot'') is prevented to participate in communication until it is cooled down, and an alternative route is generated for data transmission. This type of solution however could stop the communication for certain sources of the routing tree or even for the whole network for a particular period of time if the hotspot(s) is the only node to reach to the BC. The situation would be worse if the sources generate traffic of the utmost urgency.

The congestion problem due to non-regulated traffic is regarded as one of the most significant problems in the context of WBANs for a number of reasons. First, reliability and latency is severely affected while the congestion occurs and most of the remote health monitoring applications (e.g., ElectroCardiogram (ECG), Electroencephalogram (EEG) data) require higher reliability and timely delivery. Second, the congestion increases unnecessary retransmissions of packet and thus increases dissipated energy of the battery powered sensor nodes. Finally, the increase in useless re-transmissions also raise the temperature of the sensor nodes due to exaggerated communication.

There are numerous solutions exists in the literature which deal with the congestion problem. Most of the pioneer works present rate control solutions to mitigate congestion in the context of general Wireless Sensor Networks (WSNs) [16]–[23]. Some rate control schemes are also found in the context of WBANs [24]–[27]. Among the solutions, only one study [27] presents a rate control scheme to reduce the bioeffects in WBANs. This solution, however ignored the congestion problem. In contrast, the other solutions [24]–[26] only focused on reducing the congestion problem in WBANs. Due to the unique nature of implantable WBANs, we argue that the rate control scheme for implantable WBANs should possess the following characteristics. First and foremost, being a critical concern, the rate control scheme should consider the thermal effect. Although this problem is addressed by thermal-aware routing protocols but it could be efficiently addressed by a rate control scheme due to the ''communication down'' problem caused in thermal-aware routing protocols as mentioned before. Furthermore, as the occurrence of congestion also might cause thermal increase, hence it necessitates the development of a unified solution which could handle both the problem. Second, an implanted WBAN may include diverse body sensors with different priority. Hence, the rate control scheme should reflect this phenomena by providing a differentiated rate control of the body sensors. Finally, the rate control scheme in the context of implanted WBANs should target for congestion avoidance rather mitigating congestion upon occurrence due to its highly energy constrained and application fidelity requirements.

In this paper, we propose a differentiated rate control scheme for congestion and hotspot avoidance in implantable Wireless Body Area Networks. Our contributions are as follows:

- We present a novel receiver-based rate control scheme that concurrently considers the congestion and temperature status of a node with the aim of avoiding congestion and creation of hotspot. To the best of our knowledge, it is the first attempt that deals with both the problem in a single solution.
- We differentiated the body sensors according to the traffic it generates and define the priority of a node based on the weighted traffic flows it carries.
- We develop a sensor-centric temperature rise model that evaluates the temperature rise of a body sensor considering its traffic load.
- We propose a congestion detection scheme considering both the queue occupancy as well as traffic intensity to reflect congestion and contention level of a node.
- We provision a scheduler for propagating the traffic to the respective parent node and present a scheduling rate allocation mechanism that determines the scheduling rate reflecting the relative priority of a node.
- Finally, we evaluate the proposed method through computer simulations to determine its effectiveness.

The rest of the paper is organized as follows. We summarize the related works in section II, section III presents the system models and assumptions, the description of the proposed protocol is presented in section IV, section V provides the performance evaluation of the protocol and finally section VI concludes the paper.

II. RELATED WORKS

In the literature, a number of contributions can be found that present rate control scheme for congestion control in the context of Wireless Sensor Networks. CODA (Congestion Detection and Avoidance) [16] is one of the pioneer works in this field. It exploits both the queue length as well as channel load to detect congestion more accurately. CODA presents open-loop and closed-loop rate control strategy to address both the transient and persistent congestion. CODA controls the traffic rate using AIMD (Additive Increase Multiplicative Decrease) approach similar to the traditional TCP protocol. Congestion Control and Fairness (CCF) [17] is another earlier protocol proposed for WSNs. CCF exploits packet service time for congestion detection, and performs hop-by-hop rate control depending on the number of child nodes and the estimated service rate.

Fusion [18] blends three mechanisms operating at different layers namely hop-by-hop flow control, source rate limiting and prioritized MAC layer. Fusion detects congestion based on queue length only and exploits passive congestion notification through overhearing of the data packet by the nodes. Interference-aware Fair Rate Control [19] is another distributed rate control scheme that exploits queue length in congestion detection and notifies the congestion status through overhearing. Priority based congestion control protocol (PCCP) [20] has been proposed that detects congestion using a new metric called congestion degree which is the ratio of mean packet arrival time to the service time. PCCP employs scheduler between network and MAC layer and aims to perform effective rate adjustment by controlling scheduling rate in a hop-by-hop manner based on the current congestion degree of the parent node. PCCP also defines three priority index of a node: source priority, transit traffic priority and global priority, and considers the priority index of a node in scheduler rate adjustment as well as source rate

adjustment. Besides, a number of studies such as ESRT [21], CRRT [22], Flush [23] attempted to perform end-to-end rate control in transport layer along with reliable data delivery for WSNs.

Thermal effects of bio-implants is first studied in [7] and [8]. Considering this effect, a series of routing protocols [3], [11]–[15] have been proposed later on. Ren and Meng [27] attempted for the first time to propose a rate control scheme aiming to reduce the bio-effects of the sensor node. This study proposes a Coefficient of Absorption and Bio-effects (CAB) metric reflecting the thermal effect and presents a rate control algorithm based on this metric. The problem of allocating rate to reduce bio-effects is formulated as non-linear Network Utility Maximization problem and a price based rate control algorithm is presented to solve the problem. The solution is adopted from [28] which was originally proposed for wireless ad hoc networks. The solution however only attempts to reduce the bio-effects and ignores the congestion problem. The solution also does not consider the differentiated rate requirement of the traffic with diverse priorities. Furthermore, it requires the execution of clique construction algorithm as well as exchange of updated rate price which is not feasible for highly resource constrained WBANs.

Few solutions present the rate control scheme to control congestion in the context of WBANs. A self-adjustable rate control scheme [24] has been proposed that controls the rate of a node dynamically based on a rate prediction model. The model considers a valuation function as well as risk of congestion degree in choosing the current rate. The scheme tries to avoid the congestion by determining a suitable rate. Rezaee *et al.* [25] proposed HOCA, a Healthcare aware Optimized Congestion Avoidance and control protocol for wireless sensor networks. This proposal considers the diverse traffic types of healthcare applications and attempts to avoid congestion by distributing packets to multiple routes. The authors present a data centric active queue management scheme to prevent packet loss due to buffer overflow. Also, the solution includes a rate adjustment scheme to control the congestion when the congestion cannot be avoided through the proposed routing scheme. Recently, a congestion control solution has been proposed for WBANs mainly aiming to provide rate control for differentiated traffic of heterogeneous WBANs [26]. This solution presents a proportional fair allocation strategy for different sensor types. The paper also proposes an adaptive fair allocation approach considering different scenario in healthcare environment. The solution only considers single hop situation where the sink allocates rate to individual sensors.

The aforementioned solutions, however either focused on congestion issue or considered bioeffects of the sensors. Therefore, in this paper, we attempted to develop a unified rate control solution which aims to reduce the thermal effect of implanted bio-sensors as well as avoid congestion considering the differentiated service requirements of diverse sensor types.

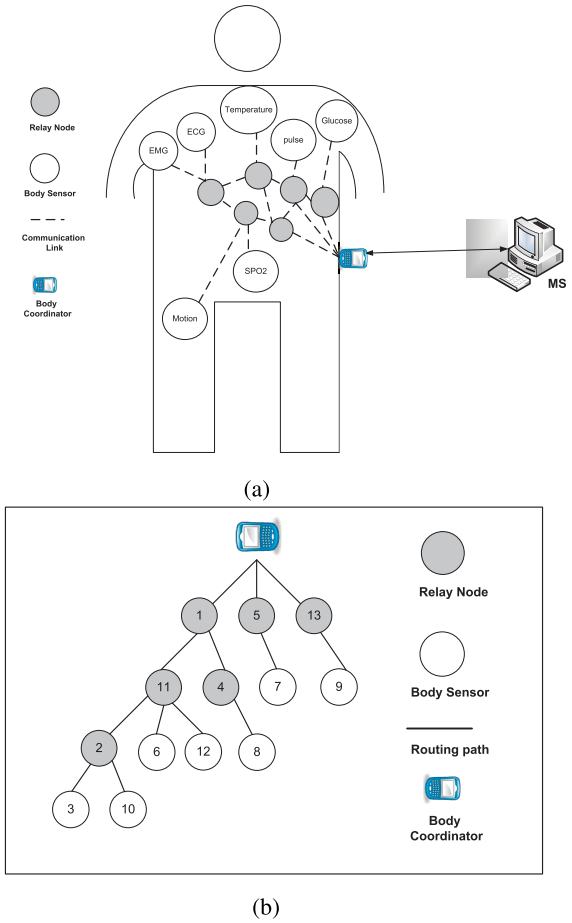

FIGURE 1. Network Model. (a) An intra-WBAN architecture. (b) A routing path established by a routing protocol.

III. SYSTEM MODELS AND ASSUMPTIONS

A. NETWORK MODEL

Figure 1 presents the considered network model, where a WBAN is formed of diverse types of implanted body sensors, a number of relay nodes, and a Body Coordinator (*BC*) that is attached to the body surface, serving as the central data sink for the WBAN. The implanted body sensors capture the physiological data such as signals from electrocardiogram (ECG), electroencephalogram (EEG) and electromyogram (EMG), SPO2, temperature etc. which will be conveyed to the medical personnel for diagnosis. We adopt the idea of using relay nodes[1] [4]–[6] to decrease the communication distance between nodes which in turn increases energy-efficiency. The implanted sensors thus forward the sensed data to a relay node, the data is then forwarded toward the *BC* in a multi-hop manner. Unlike the body sensors as well as relay nodes which are battery powered and thus energy-constrained, the *BC*, in contrast, is assumed to have an external power supply with higher processing capabilities. Upon obtaining the data

[1] Since the dimension of a WBAN is small, hence, the total number of relay nodes are usually limited. Reference [4] presents an upper limit for number of relay nodes considering path loss coefficient of different parts of the body.

from the sensors, *BC* processes it and then transmits it to a monitoring station (MS) or server through other networks (i.e., cellular, WLAN or wired) and this communication paradigm is out of the scope of this paper.

The above deployment scenario can be modeled as a connectivity graph, $\mathbf{G} = (N, E)$, where $N = \{n_1, n_2, \ldots, n_n\}$ is the set of vertices representing the nodes in the network, and E is the set of edges representing all possible communication links. We assume a routing path is already established by a routing protocol as depicted in figure 1b. However, the proposed system does not restrain in any way the routes taken by packets and thus the proposed solution is independent of the routing algorithm. When a node[2] forward a packet to the next-hop node, then the next-hop node is denoted as parent node while the forwarder is denoted as its child node. We denote the parent of a node n_j as p_{n_j} and a child of n_j as c_{n_j}. We assume that every node uses fixed transmission power and both parent and child are in the transmission range of each other.

B. QUEUING MODEL

Figure 2 illustrates the queuing model for the proposed protocol. The data generated by body sensors are divided into three traffic classes according to their priority. [3] The priority is defined considering the throughput and delay requirement of the traffic. Let TH_{C_i} and D_{C_i} denote the throughput and delay for particular class C_i. Hence, the constraints of those parameters are as follows:

$$TH_{C_1} > TH_{C_2} > TH_{C_3}$$
$$D_{C_1} < D_{C_2} < D_{C_3}$$

Following the constraints, for instance, we can assign ECG, EEG signals etc. to class-1 due to the higher throughput and lower delay requirements. Consequently, SO2, blood pressure signals are assigned to class-2, and temperature, respiration signals to class-3.

We denote the priority of a particular class, C_i as w_{C_i}. In our proposed protocol, we assign the priority values for C_1, C_2 and C_3 as 3, 2 and 1 respectively that is $w_{C_i} \in \{1, 2, 3\}$. However, assigned class for the signals is not fixed and may vary depending on critical situation or physician's requirement. In particular, a node may generate a signal exceeding a certain threshold that causes emergency situation or a physician may require certain low priority signal with higher throughput and lower delay for the purpose of accurate analysis. Hence, a dynamic assignment of the class is required to handle such situation. The assignment of the class could be initiated by the monitoring station and will be conveyed to the body sensors through the BC in a reverse path.

Each body sensor generates traffic at a particular source rate denoted as r_{sr}. For a relay node, the incoming traffic is received from its child nodes at an input rate r_{in}. When either

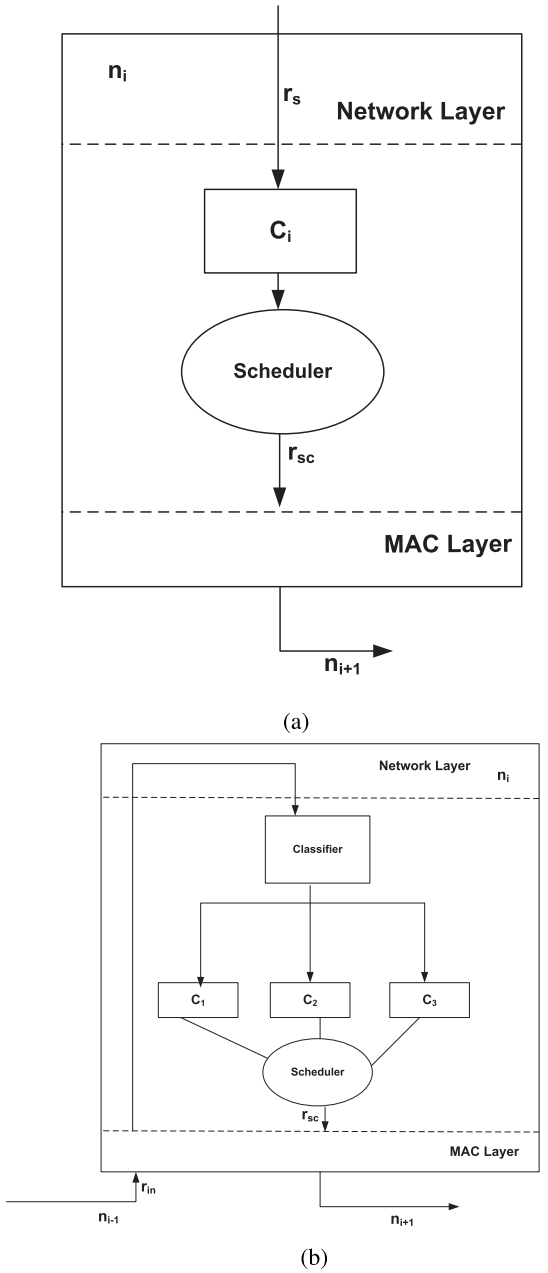

FIGURE 2. Queuing Model. (a) Queuing Model for a body sensor. (b) Queuing model for relay node.

the source rate, r_{sr} or incoming traffic rate, r_{in} exceeds the service rate, r_s at the MAC layer, packets need to be queued up and thus the congestion takes place. Similar to [20], we provision a scheduler between network layer and MAC layer. For a relay node, the scheduler maintains three queues that corresponds to three classes of traffic (figure 2a) while it maintains only one queue of a particular class C_i, $i \in \{1, 2, 3\}$ in a body sensor node (figure 2b). In a relay node, the classifier classifies the traffic and places it into the appropriate queue. The scheduler schedules the traffic from the queues at a certain rate, known as scheduling rate. We define two types of scheduling rate: required scheduling rate, $r_{rsc}^{n_j}$ of a node n_j

[2] In this paper, we use the term "node" to represent both implanted body sensor and relay node

[3] The number of classes however might vary and our protocol operation is independent of the number of traffic classes.

and effective scheduling rate, $r_{esc}^{n_j}$. The required scheduling rate, $r_{rsc}^{n_j}$ of a node n_j is defined as the rate that n_j is required to transmit to its parent node. The effective scheduling rate, $r_{esc}^{n_j}$ of a node n_j is the rate at which a node, n_j can effectively transmit data to it's parent.

We define the flow as the traffic of a particular class originating from a particular node. Hence, by definition, a body sensor can have only one flow of a particular class while a relay node may forward multiple flows of multiple traffic classes. We further define the priority of a node n_j as:

$$NP_{n_j} = \sum_{C_i} w_{C_i} \times f_{active}^{C_i} \tag{1}$$

where, f_{active}^{i} be the number of active flows for a particular class C_i. A node n_j keeps track of number of flows it forward to its parent node. If n_j does not receive a flow for a maximum time-out period, it treats the flow as inactive and update $f_{active}^{C_i}$ accordingly.

IV. PROTOCOL DESCRIPTION

A. MODELING TEMPERATURE RISE

Implanted body sensors cause temperature rise inside the human body due to communication activities including transmission and reception of packets. A number of studies [7], [8], [11] consider specific absorption rate (SAR) and Finite-Difference Time-Domain technique for modeling thermal rise. This model is tissue centric and mainly focuses on radiation from the sensor antenna and power dissipation of the sensor nodes. However, the model does not reflect the effect of offered load at a body sensor in estimating thermal rise. Thus, we develop a sensor-centric thermal-rise model considering the offered load at a body sensor. This model is termed sensor-centric as the thermal rise is observed directly from a body sensor rather considering the temperature of surrounding tissues. In this model, we make the following assumptions:

- We assume a fixed temperature rise denoted as T_r for each packet transmission or reception.
- We also assume that nodes cool down at a rate T_{cool} while it is idle or sleeping, in particular, a node is not involved in transmission or reception.

We consider each node estimates the temperature rise at a certain interval denoted as δt. Let t_{tr}^{i} and t_{rc}^{i} be the time required for transmission and reception for packet i at a sensor node respectively. Also, t_{busy} denote the total busy time of a node in transmission and reception. Hence, at each δt, t_{busy} can be estimated as:

$$t_{busy} = \sum_{i=1}^{N_t} t_{tr}^{i} + \sum_{i=1}^{N_r} t_{rc}^{i}$$

Here, N_t and N_r are the total number of packets transmitted and total number of packets received within the period δt respectively. The idle time within the interval δt, denoted as t_{idle} can also be estimated as:

$$t_{idle} = \delta t - t_{busy}$$

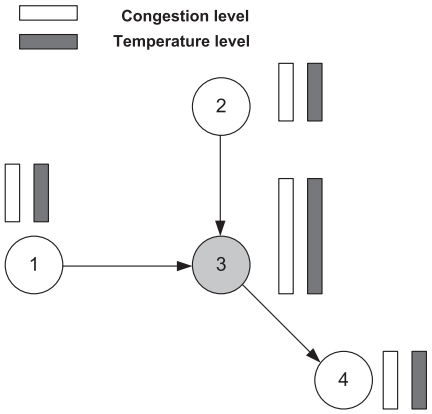

FIGURE 3. A simple WBAN of 4 nodes illustrating congestion level and thermal increase.

Let $T_{prev}^{n_j}$ be the estimated temperature at node n_j at the previous interval. Thus, the node n_j estimates the current temperature, denoted as $T_{curr}^{n_j}$ after δt as follows:

$$T_{curr}^{n_j} = T_{prev}^{n_j} + (t_{busy} \times T_{rise}) - (t_{idle} \times T_{cool}) \tag{2}$$

A node n_j identifies itself as "heated" when the current temperature $T_{curr}^{n_j}$ goes beyond some hotspot threshold, T_{th}.

B. EFFECT OF TRAFFIC LOAD ON CONGESTION AND TEMPERATURE RISE

To study the effect of traffic load on congestion and thermal increase we run a simulation consisting of four nodes as shown in figure 3. In the simulation, both node 1 and node 2 transmit traffic in different offered load through node 3 to node 4. We randomize the initial transmission time of the sources. We measure the delivery ratio and temperature at intermediate node 3. The temperature is measured using the model as explained in IV-A. The initial temperature of a node is assumed to be 37^oC.

Figure 4a presents the impact of traffic load on delivery ratio and thermal-increase measured at intermediate node 3. It is evident from the graph that after a certain offered load ($\approx$ 5 pps) congestion occurs and the delivery ratio drops dramatically. Surprisingly, we observe a thermal decrease up to a certain offered load with increasing traffic rate. It is due to the fact that, during low traffic load, a node gets sufficient time for cooling which in turn diminishes the temperature. However, while congestion occurs and channel loading increases, nodes remain busy in transmission, reception or idle listening which increases node temperature significantly with increasing offered load.

Figure 4b illustrates the time-series traces for both delivery ratio and temperature measured at intermediate node 3. In this evaluation, we set the offered load at 3.5 pps. As the figure depicts, the delivery ratio at node 3 is quite high over time (in the range of (90%-100%) due to low traffic load. However, we observe that despite the low load, the temperature increases gradually which signifies the temporal effect on thermal increase. In particular, even in the low load, a node

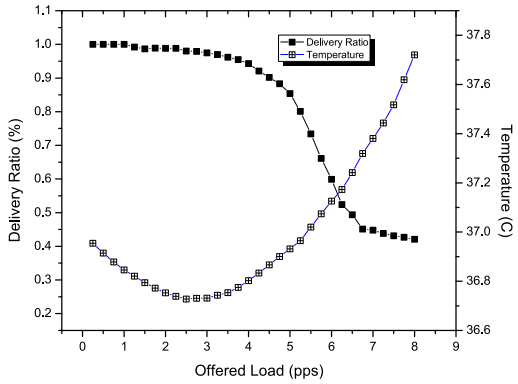

(a)

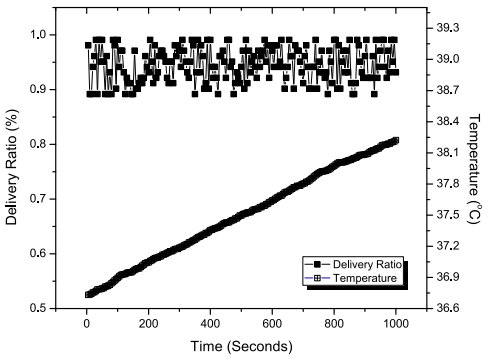

(b)

FIGURE 4. A simple simulation depicting the congestion and thermal effect. (a) Impact of traffic load on Congestion and Thermal Increase. (b) Thermal effect on low congestion situation.

TABLE 1. Status of a node based on Congestion and Temperature

Flag	Node Status
00	Not Heated, Not Congested
01	Not Heated, Congested
10	Heated, Not Congested
11	Heated, Congested

gets heated over time due to performing communication activities for a longer period.

Based on this simple simulation, we identify that a node will be in either of the four states (represented by two-bit flag) considering its congestion status and temperature as presented in table 1.

C. CONGESTION DETECTION

Most of the prior works consider queue occupancy in detecting congestion. However, the study in [16] reveals that queue occupancy alone is not sufficient for accurate and timely congestion detection. Hence, a number of protocols [16], [22] consider the combination of both queue occupancy and channel loading for efficient congestion detection, especially in hop-by-hop flow control. Following the trend, in this protocol, we take into account both queue occupancy and the level of contention for signaling the congestion.

1) QUEUE OCCUPANCY ESTIMATION

Similar to the prior works on queue occupancy based congestion detection, we adopt Exponentially Weighted Moving Average (EWMA) formula for measuring the average queue occupancy of a node n_j. As mentioned in Section III-B, a body sensor node maintains one queue for a particular class of traffic C_i where $i \in \{1, 2, 3\}$. Thus, for every packet inserted into the queue a body sensor node estimates the average queue length as follows:

$$q_{C_i}^{avg}(k+1) = (1-\alpha) \times q_{C_i}^{avg}(k) + \alpha \times q_{C_i}^{curr} \tag{3}$$

where, $q_{C_i}^{avg}(k+1)$ and $q_{C_i}^{avg}(k)$ are the average queue length for $(k+1)$th and kth packet respectively, $q_{C_i}^{curr}$ is the current queue length and $0 < \alpha < 1$ is the tuning parameter.

A relay node, on the other hand, maintains multiple queues for multiple classes of traffic. Let ω_i be the weight of a particular queue i. The weight of the queue is assigned as per the priority value of the corresponding class. A relay node estimates average queue length for every queue according to equation 3. Thus, we define the weighted average queue length, $\overline{q^{avg}}$ as:

$$\overline{q^{avg}} = \frac{\sum_i \omega_i \times q_{C_i}^{avg}}{\sum_i \omega_i}, i \in \{1, 2, 3\} \tag{4}$$

2) CONTENTION MEASUREMENT BASED ON TRAFFIC INTENSITY

We define the traffic intensity, ρ_{n_j} for a node n_j as:

$$\rho^{n_j} = \frac{r_a^{n_j}}{r_s^{n_j}} \tag{5}$$

where, $r_a^{n_j}$ and $r_s^{n_j}$ are the packet arrival rate and packet service rate at node n_j respectively. The $r_a^{n_j}$ and $r_s^{n_j}$ can be derived as:

$$r_a^{n_j} = \frac{1}{t_a^{n_j}}$$
$$r_s^{n_j} = \frac{1}{t_s^{n_j}} \tag{6}$$

Here, $t_a^{n_j}$ and $t_s^{n_j}$ denote the average packet inter-arrival time and average packet service time respectively.

Average packet inter-arrival time, $t_a^{n_j}$ is the time interval between two successively arriving packets at the MAC layer. For each packet arrival at the MAC layer, $t_a^{n_j}$ is updated as follows:

$$t_a^{n_j} \leftarrow \frac{t_a^{n_j} \times n + t_a^{last}}{n+1} \tag{7}$$
$$n \leftarrow n+1 \tag{8}$$

where, t_a^{last} is the inter-arrival time of the most recently arrived packet and n denote a counter specifying the number of packets over which the average value will be measured.

We define the packet service time is the time elapsed between a packet arrives at the MAC layer and when the packet has been successfully transmitted. It includes the time for MAC layer contention resolution, and packet transmission delay. Similar to equation 7 and 8 we measure the average packet service time as:

$$t_s^{n_j} \leftarrow \frac{t_s^{n_j} \times n + t_s^{last}}{n+1} \tag{9}$$

$$n \leftarrow n+1 \tag{10}$$

where, t_s^{last} is the service time of the most recently transmitted packet. In our implementation, we choose the iteration duration is 100 packets. In particular, the average packet inter-arrival time or average packet service time will be reset after the arrival of 100 packets. The traffic intensity provides good indication on contention level surrounding a node. The decrease in packet service rate increases the traffic intensity. A value of $\rho_{n_j} > 1$ indicates severe contention or high channel load while the packet service rate falls below the packet arrival rate.

3) SIGNALING CONGESTION

A node n_j signals for congestion when the estimated average queue occupancy and the traffic intensity exceeds some watermark level. In particular, we exploit two thresholds q_{th} and ρ_{th} representing queue occupancy threshold and traffic intensity threshold respectively. The congestion is detected when $q_{C_i}^{avg} > q_{th}$ (for a body sensor) or $\overline{q^{avg}} > q_{th}$ (for relay node), and $\rho^{n_j} > \rho_{th}$.

D. PROPAGATION OF CONTROL INFORMATION

The protocol requires dissemination of a number of control information for effective rate adjustment. Since, sending additional control packet contributes to congestion as well as temperature increase, following the trend of earlier approaches [19], [20], we piggy-back the control information on data packets. Exploiting the broadcast nature of a wireless channel, a child node overhears the data packet sent by the parent node. A node n_j includes the following information in the data packet header. i) node status represented by two-bit flag (table 1), ii) node priority, NP_{n_j}, and iii) receivable rate, $r_{rc}^{n_j}$. We define the receivable rate for a node n_j is the maximum allowable rate at which n_j receive packets from its child nodes. To reduce the overhead, the notification is triggered when a change occurs in any of the information instead of sending the information in each data packet.

E. RECEIVABLE RATE ADJUSTMENT

As defined in the previous section, the receivable rate, $r_{rc}^{n_j}$ determines the maximum allowable rate that the receiver can receive from its child nodes. In this paper, we propose a receiver-driven rate control mechanism where a node n_j chooses an optimal $r_{rc}^{n_j}$ considering it's congestion status and ''thermal'' condition. We present the procedure for receivable rate adjustment in algorithm 1.

begin
  INPUT: $r_{rsc}^{n_j}$, $r_s^{n_j}$, *status*,
  switch *status* **do**
    case
      00
    end
    $r_{rc}^{n_j} = \min\ (r_{rsc}^{n_j}, r_s^{n_j})$ **case** 01
      $r_{rc}^{n_j} = \min\ (r_{rsc}^{n_j}, r_s^{n_j})$
      $r_{rc}^{n_j} = (1-\beta) \times r_{rc}^{n_j}$
    end
    case 10 *or* 11
      $T_{curr}^{n_j} = GetCurrentTemp()$;
      while $T_{curr}^{n_j} > (1-\gamma) \times T_{th}$ **do**
        $r_{rc}^{n_j} = r_{rc}^{0}$
        $T_{curr}^{n_j} = GetCurrentTemp()$;
      end
    end
  endsw
end

Algorithm 1 Receivable rate Adjustment at n_j

The algorithm takes the current required scheduling rate $r_{rsc}^{n_j}$, packet service rate, $r_s^{n_j}$ and current node status (table 1) as input, and considers three cases in adjusting the receivable rate. The determination of $r_{rsc}^{n_j}$ will be discussed in section IV-F.

- First, when the node is in state ''00'' that is, ''not heated, not congested'', it tries to utilize the capacity as maximum as possible. However, if the capacity of the node is higher than its required scheduling rate and the node chooses its receiving rate to its capacity, then it would cause congestion at the node itself. On the other hand, when the capacity of the node is less than its required scheduling rate, then the node must chooses it's receiving rate as per the capacity. Hence, a node n_j determines its receiving rate as the minimum of its required scheduling rate and packet service rate.
- Second, during ''not heated but congested'' state (01), a node reduces its receiving rate to a slightly lower value which is controlled by the factor β. The main aim is to keep the packet service rate greater than the receiving rate to alleviate the congestion.
- Finally, at the time of ''heated'' state (either 10 or 11) irrespective of the congestion status, a node keeps the current receiving rate to a base value, r_{rc}^{0} unless the current temperature falls below some factor of the hotspot threshold, T_{th}. The rationale behind maintaining a very lower receiving rate, r_{rc}^{0} at that state is due to the observation depicted in figure 4a as discussed earlier in section IV-B which signifies the gradual decrease in node temperature at a low traffic load. Although, keeping a lower receiving rate results poor channel utilization, however, mitigating the ''heated'' state is the foremost consideration to prevent tissue damage.

Moreover, a heated node also could be used for transmitting higher priority data rather ignoring it completely.

F. SCHEDULING AND SOURCE RATE ALLOCATION

As explained in section III, our protocol exploits two types of scheduling rate, required scheduling rate, $r_{rsc}^{n_j}$ and effective scheduling rate, $r_{esc}^{n_j}$. The required scheduling rate allocation mainly depends on two factors: i) receivable rate of the parent node and ii) the priority of a node and its parent node. Let $r_{rc}^{p_{n_j}}$ denote the receivable rate of the parent node of node n_j and $NP_{p_{n_j}}$ be the node priority of the parent of node n_j . Hence, the required scheduling rate of a node, $r_{rsc}^{n_j}$ is estimated as:

$$r_{rsc}^{n_j} = \frac{NP_{n_j}}{NP_{p_{n_j}}} \times r_{rc}^{p_{n_j}} \tag{11}$$

Thus the required scheduling rate is determined based on the relative priority of the node which in turn depends on weighted active flows. This signifies that a node having higher weighted flows will have more share to the receivable rate of its parent. A node obtains the receivable rate and priority of its parent node according to IV-D.

The effective scheduling rate, $r_{esc}^{n_j}$ reflects the actual rate that the node can forward to its parent. To avoid the congestion, we assign its receivable rate to effective scheduling rate. Hence,

$$r_{esc}^{n_j} = r_{rc}^{n_j}$$

Whenever a parent node falls into the ''heated'' state, the receivable rate is reduced to a base rate as discussed in the previous section. In this situation, it is desirable to pass only higher priority traffic (C_1) through this heated parent node. Hence, whenever a node turns into a ''heated'' node it re-evaluates its priority value by assigning $w_{C_i} = 0$ for $i \in \{2, 3\}$. Upon being notified of the ''heated'' status of the parent node, a node n_j also re-estimates its priority value following the same way. However, after turning back to the ''non-heated'' state, a node along with its corresponding child nodes estimate their priority value in a regular manner as discussed in section III-B.

In our network model, the source nodes are only body sensor nodes and they are leaf nodes in the routing tree. Hence, the term ''receivable rate'' is not applied for source nodes as these nodes act as originators only. However, since the source node needs to originate traffic as per its effective scheduling rate, thus the same mechanism as used for measuring receivable rate will be used for determining the source rate. Therefore, a body sensor determines its source rate as:

$$r_{sr}^{n_j} = \min(r_{rsc}^{n_j}, r_s^{n_j})$$

Moreover, there is a possibility of source node itself being congested and heated. In that case, the source rate will be determined in the same way as the receivable rate is measured in the congestion state and heated state.

TABLE 2. Parameters and their values used in the simulation

Parameter	Value	Parameter	Value
Temperature rise, T_r	0.1^oC	Cooling rate, T_{cool}	$0.01^oC/s$
α	0.05	n	200 packets
β	0.1	γ	0.025
δ_t	5s	r_{rc}^0	0.5pps
Each Queue length	10 packets	q_{th}	4 packets
T_{th}	38.5^oC	ρ_{th}	0.9
MAC protocol	802.15.4	Data rate	250 kbps
Radio range	2m	Payload size	32 bytes
Retry limit	5	Simulation time	1000s

V. PERFORMANCE EVALUATION

In this section, we present the performance of the proposed rate control mechanism. The performance is evaluated using C++ based simulations.

A. SIMULATION ENVIRONMENT

A network area of $10m \times 10m$ is used where 13 nodes are deployed in uniform random distribution. We use the topology as shown in figure 1b where static routing paths[4] are used between each sensor node to the sink. In this topology 7 nodes act as source nodes and the remaining 6 nodes are relay nodes. Sources are of different priority and generate traffic periodically. We assume node 10 (ECG) and 8 (EEG) generate C_1 traffic, node 3 (SO2) and 7 (blood pressure) generate C_2 traffic and node 6 (temperature), 12 (respiration) and 9 (heart rate) are generating C_3 traffic with constant bit rate. The initial temperature is set to 37^oC. The initial data generation by the source nodes is randomized to avoid synchronized periodic reports. Basic functionalities of IEEE 802.15.4 MAC protocol non-beacon enabled mode [29] was used with its default parameters as mentioned in the standard. In the graphs, packets refer to only data packets. The results are averaged over 10 runs. Table 2 presents the detailed simulation parameters.

B. PERFORMANCE METRICS

To evaluate the proposed protocol, the following metrics are used.

Average Temperature increase. The average temperature increase denotes the average increase in temperature of a node with respect to its initial temperature.

Maximum Temperature increase. Maximum temperature increase presents the highest temperature increase of any node in a WBAN.

Normalized Throughput. This metric is defined as the ratio of the current throughput of a node or a particular traffic class or total throughput received at the BC to the system maximum throughput, and the system maximum throughput is normalized to 1.

Packet loss rate. The packet loss rate illustrates the ratio of the total number of packet drops to the total number of transmitted packets (including retransmissions).

[4]We considered an implanted WBAN where nodes are static and intended to measure the performance of the proposed protocol irrespective of any routing protocol

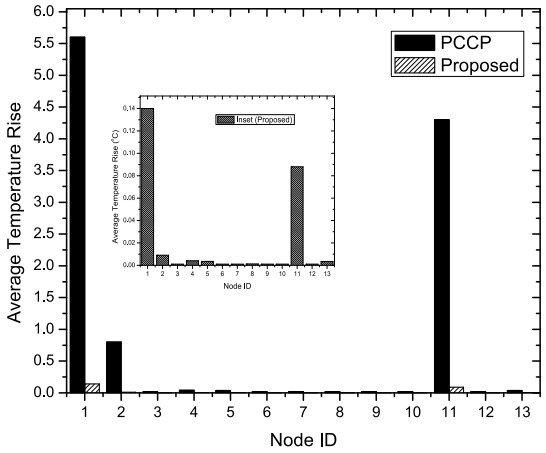

FIGURE 5. Average temperature rise of the nodes.

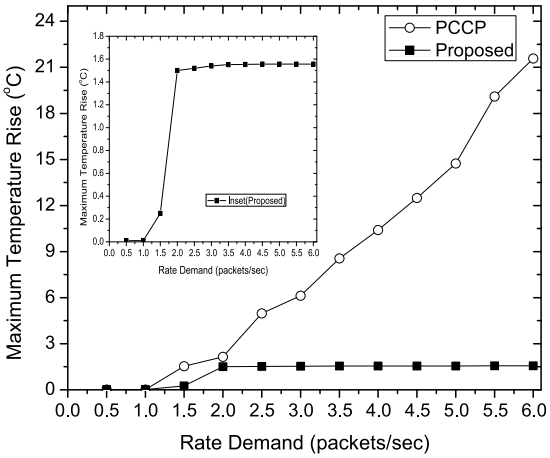

FIGURE 6. Maximum temperature rise with increasing rate demand.

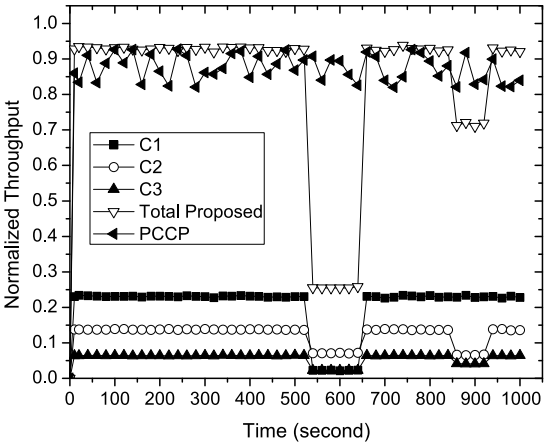

FIGURE 7. Normalized throughput of different traffic class of the proposed protocol, total throughput of the proposed protocol and the PCCP.

Network efficiency. We define the network efficiency, η [18] as:

$$\eta = \frac{\sum_{u \in U} hop(u)}{\sum_{p \in P} \sum_{h \in hop(p)} ntrnsm(p, h)} \tag{12}$$

where, U is the set of successfully received packets by the BC, P is the set of data packets generated by the sensors, hop(p) denotes the hop count the packet takes, ntrnsm(p,h) denotes the number of transmissions packet p takes at each hop.

End-to-End Latency. This metric measures the average delay incurred between the time a packet is originated to the time it is received by the BC. The value is averaged over the sum packet reception by the BC.

Average Energy Consumption This parameter reflects the average energy consumption of the nodes because of transmission and reception of data packets. In the experiment, we consider 0.2 units of energy depletion for each transmission and 0.1 unit for reception.

C. SIMULATION RESULTS

1) TEMPERATURE PERFORMANCE

We evaluate the effect of the rate control schemes on temperature rise of the nodes. The average increase of temperature of the nodes is depicted in figure 5. The main figure compares the average temperature rise for both PCCP and the proposed protocol. The inset shows the average temperature rise for the proposed protocol as there is significant performance gap between these two protocols for some nodes. As the figure illustrates, the temperature rise mainly depends on the number of flows a node carries. This is obvious because the more time a node involves in communication will affect the temperature rise. Hence, the relay nodes show comparatively higher temperature rise than the source nodes. Therefore, node 1 has the highest average temperature rise for both the protocols due to its involvement in propagating maximum number of flows (5 flows). However, due to temperature-aware rate control, the proposed protocol shows considerably better performance than PCCP in average temperature rise for all the nodes, although the performance gap is mainly observed for the relay nodes having higher active flows (node 1 and node 11).

Figure 6 depicts the maximum temperature rise for any node with increasing rate demand. The lack of thermal-awareness in rate control scheme causes a dramatic increase of temperature rise for PCCP after a certain offered load (1.5 pps) which signifies that such rate control scheme cannot be adopted in intra-BAN scenario. The maximum temperature of a node also increases with the increasing rate demand for the proposed protocol. However, after a certain rate demand (1.5 pps), the maximum temperature rise is found to be stable at 1.5^oC (inset figure) since the proposed rate control scheme prevents the node temperature exceeding the hotspot threshold limit.

2) THROUGHPUT PERFORMANCE

Figure 7 compares the normalized throughput of different traffic classes of the proposed protocol, the total throughput of the proposed protocol and the PCCP. As the figure shows, each of the traffic class achieves throughput nearly as per

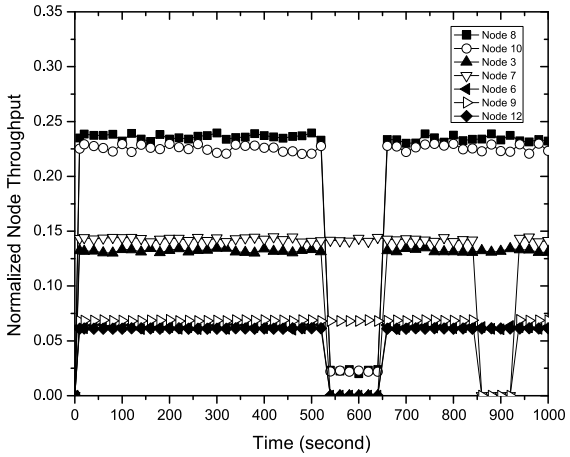

FIGURE 8. Normalized node throughput of the proposed protocol.

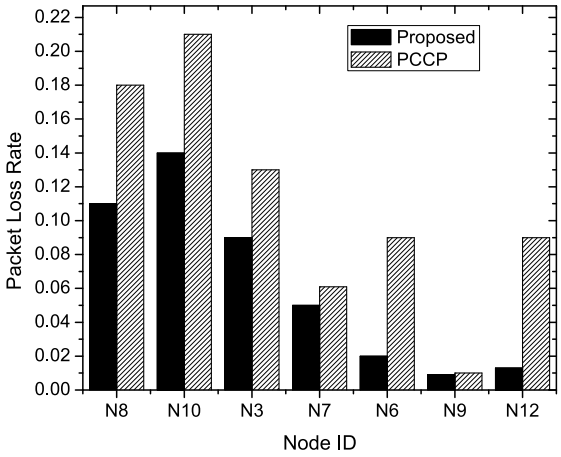

FIGURE 9. Packet Loss Rate for different sources.

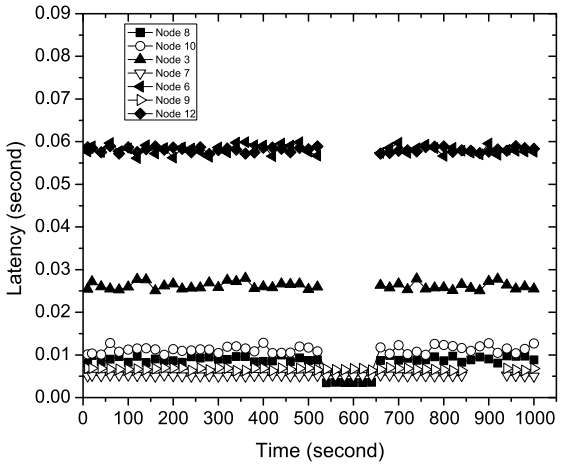

FIGURE 10. End-to-End Latency for different nodes.

its assigned weight. However, during the periods between 540 - 650 second and 850-940 second, we observe a decline in throughput for the traffic classes. This is due to the highly conservative rate reduction while a node crosses the hotspot threshold. To compare the throughput performance between PCCP and the proposed protocol, we plot the total throughput of both the protocols. Both the PCCP and the proposed protocol achieves higher throughput. However, due to the rate reduction policy during the heated state, the throughput of the proposed protocol drops in some periods. Although PCCP maintains higher throughput throughout the period, but it comes with the compensation of excessive thermal rise as discussed earlier.

The normalized node throughput of the proposed protocol is portrayed in figure 8. Being the sources of C_1 traffic class, node 8 and node 10 achieve the highest throughput (0.23 on average) compared to the other nodes. As a generator of C_2 traffic class, node 3 and node 7 obtain the average throughput of 0.135, and the remaining nodes (node 6. 9 and 12) of C_1 traffic class achieve the lowest throughput (0.063 on average). During the period $540 - 650$ second, the throughput of node 3, 10, 6, 12 and 8 drops significantly. At this period, the relay node 1 and 11 gets heated and the temperature crosses the hotspot threshold. It causes the rate reduction to the basic rate. However, even in this heated situation, node 8 and node 10 as the sources of C_1 traffic class, obtain throughput at a minimum level (0.023 on average), whereas the node 3, 6 and 12 achieve no throughput. At this period, node 7 and node 9 obtain their desired throughput as per assigned weight since no node on the path of those flows gets heated. However, at the period of 850-940 second, we observe nearly zero throughput for those flows as their respective parents (node 5 and 13) became hotspot during that time.

3) PACKET LOSS RATE

The packet loss rate performance for both PCCP and the proposed protocol is portrayed in figure 9. All the traffic sources show better performance in achieving low packet loss rate for the proposed protocol than PCCP. This is because of the effective congestion detection mechanism of the proposed protocol that considers both queue occupancy and traffic intensity. Moreover, the receiving rate adjustment procedure of the proposed protocol reflects the suitable rate a node can receive from its child nodes which depends on the required scheduling rate and measured capacity. Interestingly, higher priority sources (node 8, node 10) suffer from higher loss rate. This is due to the generation of more traffic from those sources and transmitted through the relay nodes. PCCP suffers higher loss rate in all sources as the rate adjustment procedure of PCCP only considers the parent congestion degree. However, if the grandparent of a node gets congested, but the congestion degree of the parent is still smaller, the child nodes will keep increasing their rates to the parent which will cause congestion and packet loss at the parent node.

4) LATENCY PERFORMANCE

The average end-to-end latency for different nodes of different traffic classes is illustrated in figure 10. As the figure shows, the latency performance not only depends on the

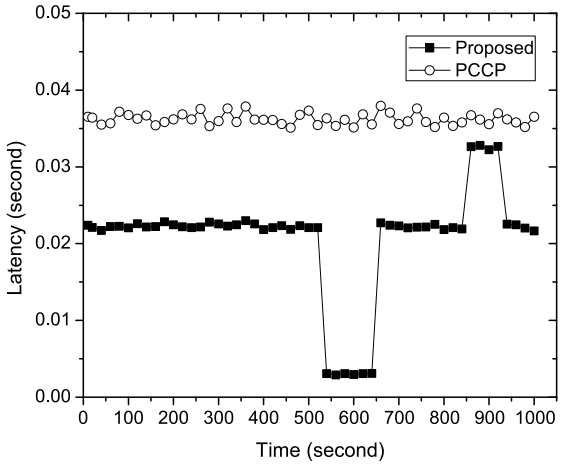

FIGURE 11. Latency performance between PCCP and the Proposed protocol.

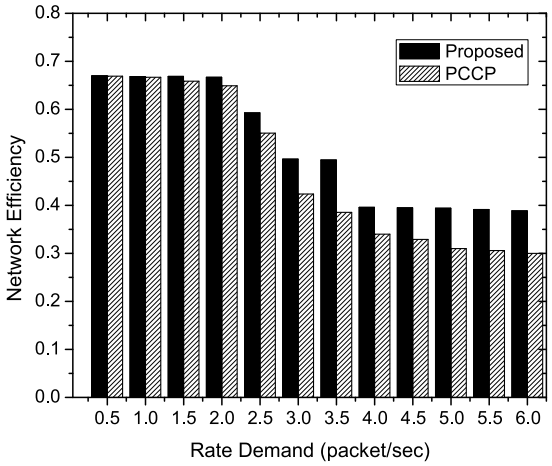

FIGURE 12. Network Efficiency under varying rate demands.

traffic priority but also its position in the routing tree. Being the sources of C_1 traffic type both node 8 and node 10 show lower latency performance. As a C_2 traffic generator, node 3 depicts a bit higher latency performance than node 8 and 10. Despite being a source of C_2 traffic, the latency performance of node 7 is better than node 3 as it is just two hops away from the *BC* and its parent node (node 5) relays only the traffic of node 7. For the same reason node 9 also shows better latency performance even though it is a source of C_3 traffic while the latency performance of node 6 and 12 is the worst among all due to their lower traffic priority as well as their position in the routing tree. These traffic flows have to contend with the flows of other higher priority traffic classes, and their corresponding relay nodes (node 11 and node 1) also carry traffic from all the traffic classes. Besides, we observe during the period 540-650 second , there is no traffic for node 3, 6, 12 due to the existence of hotspot node on their path to the *BC*, and hence the gap. Similar situation is observed for node 7 and 9 during the period 850-940.

We compare the average end-to-end latency performance of PCCP and the proposed protocol in figure 11. As depicted in the figure, throughput the period the latency performance of the proposed protocol is better than PCCP. The factors such as lower contention, lower packet loss rate as well as maintaining lower queue length through effective rate control contribute to such lower end-to-end latency of the proposed protocol. Due to the rate control policy during hotspot, we observe some notable fluctuations in the latency performance of the proposed protocol. In some period such as 540-650 second , the latency drops significantly since at this period the traffic from lower priority classes have been stopped which reduces contention as well as queue length to a great extent resulting in lower average latency. However, as we explained in figure 11, at the period between 850-940 second node 7 and 9 stops generating traffic due to the formation of hotspot of their respective relay nodes. As the latency performance of these two traffic flows are usually better hence preventing them in sourcing traffic influences in increasing the average end-to-end latency of the proposed protocol during that period.

5) NETWORK EFFICIENCY

We evaluate the network efficiency under different rate demands as illustrated in figure 12. Since, we consider the static routing path, hence the network efficiency mainly depends on the number of successfully received packets as well as the number of retransmission at each hop. As the figure shows, while the rate demand at the sources are lower, in particular during low traffic load, both the proposed protocol and PCCP exhibit higher network efficiency. However, the efficiency reduces with increasing rate demand due to the growing loss rate and number of retransmissions. Yet, the proposed protocols shows comparatively better performance than PCCP at high rate demands due to its lower loss rate and reduced number of retransmissions per hop through its effective rate adjustment scheme.

6) ENERGY PERFORMANCE

Figure 13 compares the average energy consumption of the protocols for different nodes. Clearly, the average energy consumption of the nodes having higher number of offspring is much higher than the nodes with lower offspring or the source nodes. Hence, node 1 and 11 have significantly higher energy consumption than the other nodes for both the protocols. The source nodes that generate higher priority traffic also depicts slightly higher energy consumption than lower priority sources due to the differences in amount of traffic generation. For all the nodes, the proposed protocol excels PCCP in achieving lower energy consumption since its receivable rate adjustment procedure effectively determines the receivable rate considering the required scheduling rate to the parent node as well as its measured network capacity. This results lower loss rate and retransmission which in turn lowers the energy consumption. Moreover, at the heated situation, the proposed protocol allows only higher priority traffic class

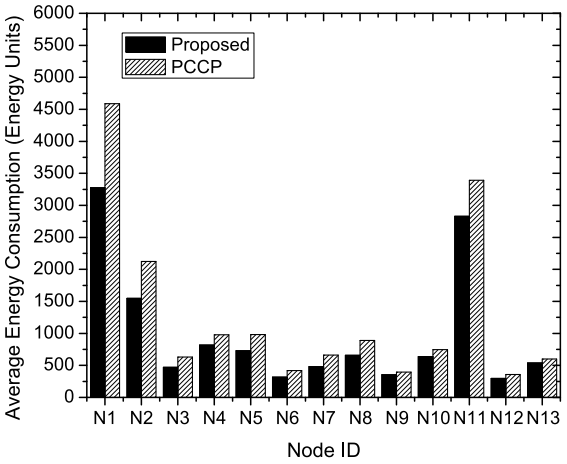

FIGURE 13. Average Energy Consumption for different nodes.

generating traffic in a very low rate, also prevents nodes having other traffic classes in sourcing traffic which also contributes to the lower energy consumption.

VI. CONCLUSION

In this paper, we have presented a novel rate control scheme targeting to provide a unified solution for congestion and hotspot avoidance in implantable WBANs. The proposed scheme detects congestion considering both queue occupancy along with traffic intensity to accurately measure the level of congestion in a node. It also presents a sensor-centric temperature rise model to measure node temperature based on its traffic load. Moreover, the solution considers the traffic differentiation according to their throughput and latency demands, and present a scheduling rate allocation mechanism reflecting the node priority index.

We have evaluated the protocol performance through simulations and compared the performance with PCCP. The results demonstrated that the proposed scheme can successfully maintain lower temperature rise throughout the network as well as avoid the creation of hotspot(s) in any traffic load. Moreover, the results indicated that the scheme can improve the performance of healthcare applications in achieving higher and weighted fair throughput, reducing packet loss rate, attaining lower end-to-end latency, and obtaining higher network efficiency along with lower energy consumption.

ACKNOWLEDGMENTS

The authors, therefore, gratefully acknowledge the DSR technical support.

REFERENCES

[1] B. Warneke and K. S. Pister, "MEMS for distributed wireless sensor networks," in *Proc. 9th IEEE Int. Conf. Electron., Circuits Syst.*, vol. 1. Sep. 2003, pp. 291–294.

[2] M. Chen, S. Gonzalez, A. Vasilakos, H. Cao, and V. C. M. Leung, "Body area networks: A survey," *Mobile Netw. Appl.*, vol. 16, no. 2, pp. 171–193, 2011.

[3] A. Bag and M. A. Bassiouni, "Energy efficient thermal aware routing algorithms for embedded biomedical sensor networks," in *Proc. IEEE Int. Conf. Mobile Ad Hoc Sensor Syst. (MASS)*, Oct. 2006, pp. 604–609.

[4] A. Ehyaie, M. Hashemi, and P. Khadivi, "Using relay network to increase life time in wireless body area sensor networks," in *Proc. IEEE Int. Symp. World Wireless, Mobile Multimedia Netw. Workshops*, Jun. 2009, pp. 1–6.

[5] N. Javaid, A. Ahmad, Y. Khan, Z. A. Khan, and T. A. Alghamdi, "A relay based routing protocol for wireless in-body sensor networks," *Wireless Pers. Commun.*, vol. 80, no. 3, pp. 1063–1078, Feb. 2015. [Online]. Available: http://dx.doi.org/10.1007/s11277-014-2071-x

[6] J. I. Bangash, A. H. Abdullah, M. A. Razzaque, and A. W. Khan, "Reliability aware routing for intra-wireless body sensor networks," *Int. J. Distrib. Sensor Netw.*, vol. 10, no. 10, p. 786537, 2014. [Online]. Available: http://dx.doi.org/10.1155/2014/786537

[7] G. Lazzi, "Thermal effects of bioimplants," *IEEE Eng. Med. Biol. Mag.*, vol. 24, no. 5, pp. 75–81, Sep. 2005.

[8] Q. Tang, N. Tummala, S. K. S. Gupta, and L. Schwiebert, "Communication scheduling to minimize thermal effects of implanted biosensor networks in homogeneous tissue," *IEEE Trans. Biomed. Eng.*, vol. 52, no. 7, pp. 1285–1294, Jul. 2005.

[9] L. Schwiebert, S. K. S. Gupta, P. S. G. Auner, G. Abrams, R. Iezzi, and P. McAllister, "A biomedical smart sensor for the visually impaired," in *Proc. IEEE Sensors*, vol. 1. Sep. 2002, pp. 693–698.

[10] A. Hirata, G. Ushio, and T. Shiozawa, "Calculation of temperature rises in the human eye exposed to em waves in the ism frequency bands(special issue on recent progress in electromagnetic compatibility technology)," *IEICE Trans. Commun.*, vol. 83, no. 3, pp. 541–548, Mar. 2000. [Online]. Available: http://ci.nii.ac.jp/naid/110003218659/en/

[11] Q. Tang, N. Tummala, S. Gupta, and L. Schwiebert, "Tara: Thermal-aware routing algorithm for implanted sensor networks," in *Distributed Computing in Sensor Systems* (Lecture Notes in Computer Science), vol. 3560, V. Prasanna, S. Iyengar, P. Spirakis, and M. Welsh, Eds. Berlin, Germany: Springer, 2005, pp. 206–217.

[12] D. Takahashi, Y. Xiao, F. Hu, J. Chen, and Y. Sun, "Temperature-aware routing for telemedicine applications in embedded biomedical sensor networks," *EURASIP J. Wireless Commun. Netw.*, vol. 2008, pp. 26:1–26:26, Jan. 2008. [Online]. Available: http://dx.doi.org/10.1155/2008/572636

[13] A. Bag and M. Bassiouni, "Hotspot preventing routing algorithm for delay-sensitive biomedical sensor networks," in *Proc. IEEE Int. Conf. Portable Inf. Devices, (PORTABLE)*, Sep. 2007, pp. 604–609.

[14] M. M. Monowar, M. M. Hassan, F. Bajaber, M. A. Hamid, and A. Alamri, "Thermal-aware multiconstrained intrabody QoS routing for wireless body area networks," *Int. J. Distrib. Sensor Netw.*, vol. 2014, no. 676312, p. 14, 2014.

[15] M. M. Monowar and F. Bajaber, "On designing thermal-aware localized QOS routing protocol for *in-vivo* sensor nodes in wireless body area networks," *Sensors*, vol. 15, no. 6, pp. 14016–14044, 2015. [Online]. Available: http://www.mdpi.com/1424-8220/15/6/14016

[16] C.-Y. Wan, S. B. Eisenman, and A. T. Campbell, "Coda: Congestion detection and avoidance in sensor networks," in *Proc. 1st Int. Conf. Embedded Netw. Sensor Syst.*, New York, NY, USA, 2003, pp. 266–279. [Online]. Available: http://doi.acm.org/10.1145/958491.958523

[17] S. Brahma, M. Chatterjee, and K. Kwiat, "Congestion control and fairness in wireless sensor networks," in *Proc. 8th IEEE Int. Conf. Pervas. Comput. Commun. Workshops (PERCOM Workshops)*, Mar. 2010, pp. 413–418.

[18] B. Hull, K. Jamieson, and H. Balakrishnan, "Mitigating congestion in wireless sensor networks," in *Proc. 2nd Int. Conf. Embedded Netw. Sensor Syst.*, New York, NY, USA, 2004, pp. 134–147. [Online]. Available: http://doi.acm.org/10.1145/1031495.1031512

[19] S. Rangwala, R. Gummadi, R. Govindan, and K. Psounis, "Interference-aware fair rate control in wireless sensor networks," *SIGCOMM Comput. Commun. Rev.*, vol. 36, no. 4, pp. 63–74, Aug. 2006. [Online]. Available: http://doi.acm.org/10.1145/1151659.1159922

[20] C. Wang, B. Li, K. Sohraby, M. Daneshmand, and Y. Hu, "Upstream congestion control in wireless sensor networks through cross-layer optimization," *IEEE J. Sel. Areas Commun.*, vol. 25, no. 4, pp. 786–795, May 2007.

[21] Y. Sankarasubramaniam, O. B. Akan, and I. F. Akyildiz, "Esrt: Event-to-sink reliable transport in wireless sensor networks," in *Proc. 4th ACM Int. Symp. Mobile Ad Hoc Netw. Comput.*, New York, NY, USA, 2003, pp. 177–188. [Online]. Available: http://doi.acm.org/10.1145/778415.778437

[22] M. M. Alam and C. S. Hong, "Crrt: Congestion-aware and rate-controlled reliable transport in wireless sensor networks," *IEICE Trans. Commun.*, vol. 92-B, no. 1, pp. 184–199, 2009.

[23] S. Kim *et al.*, "Flush: A reliable bulk transport protocol for multihop wireless networks," in *Proc. 5th Int. Conf. Embedded Netw. Sensor Syst.*, New York, NY, USA, 2007, pp. 351–365. [Online]. Available: http://doi.acm.org/10.1145/1322263.1322296

[24] Y. M. Baek, B. H. Lee, J. Yun, K. Cho, and K. Han, "A self-adjustable rate control in wireless body area networks," in *Proc. 1st Int. Conf. Netw. Commun.*, Dec. 2009, pp. 404–407.

[25] A. A. Rezaee, M. H. Yaghmaee, A. M. Rahmani, and A. H. Mohajerzadeh, "Hoca: Healthcare aware optimized congestion avoidance and control protocol for wireless sensor networks," *J. Netw. Comput. Appl.*, vol. 37, pp. 216–228, Jan. 2014. [Online]. Available: http://dx.doi.org/10.1016/j.jnca.2013.02.014

[26] S. Manfredi, "Congestion control for differentiated healthcare service delivery in emerging heterogeneous wireless body area networks," *IEEE Wireless Commun.*, vol. 21, no. 2, pp. 81–90, Apr. 2014.

[27] H. Ren and M. Q. H. Meng, "Rate control to reduce bioeffects in wireless biomedical sensor networks," in *Proc. 3rd Annu. Int. Conf. Mobile Ubiquitous Syst. Workshops*, Jul. 2006, pp. 1–7.

[28] Y. Xue, B. Li, and K. Nahrstedt, "Optimal resource allocation in wireless ad hoc networks: A price-based approach," *IEEE Trans. Mobile Comput.*, vol. 5, no. 4, pp. 347–364, Apr. 2006.

[29] *Wireless Medium Access Controls (MAC) and Physical Layer (phy) Specifications for Low-Rate Wireless Personal Area Networks (WPANS)*, IEEE standard 802.15.4-2003, 2003.

MUHAMMAD MOSTAFA MONOWAR received the B.Sc. degree in computer science and information technology from the Islamic University of Technology, Bangladesh, in 2003, and the Ph.D. degree in computer engineering from Kyung Hee University, South Korea, in 2011. He was a Faculty Member with the Department of Computer Science and Engineering, University of Chittagong, Bangladesh. He is currently an Assistant Professor with the Department of Information Technology, King Abdulaziz University, Saudi Arabia. His research interests include wireless networks, especially ad hoc, sensor and mesh networks, including routing protocols, MAC mechanisms, IP and transport layer issues, cross-layer design, and QoS provisioning.

FUAD BAJABER received the B.S. degree in computer science from King Abdulaziz University (KAU), Saudi Arabia, the M.S. degree in computer science from George Washington University, USA, and the Ph.D. degree from the Department of Computing, Bradford University, U.K. Prior to pursuing his Ph.D., he was a Senior Systems Engineer with KAU. He is currently an Assistant Professor with the Department of Information Technology, KAU. His main research interests include design, analysis and measurement of wireless sensor and adhoc networks and cloud computing.